



BIU-YU Summer Research Internship 2016



Program Director:
Prof. Ari Zivotofsky
Av & Em Bayit:
Isaac & Tal Attia

The BIU-YU Summer Science Research Internship program enables talented undergraduate students to take part in research at one of Bar-Ilan's distinguished laboratories. Through the generous support of Bar-Ilan's Global Board of Trustees Chairman, Dr. Mordecai D. Katz, and his wife Dr. Monique Katz, and by the J. Samuel Harwit, zt"l & Manya Harwit Aviv Charitable Trust participants are able to gain research experience and develop laboratory skills, all while being exposed to Israeli science, technology, and culture.

Table of Contents

Mathematics & Engineering

| | |
|---|---|
| Tamar Felman :: Prof. Sharon Ganot. | 3 |
| Ben Kaplan & Sara Palgon :: Prof. Rachela Popovtzer. | 4 |
| Andrew Katz :: Prof. Dror Fixler. | 5 |
| Daniel Klovsky :: Prof. Yuval Roichman & Prof. Ron Adin. | 5 |
| Brian Snow :: Dr. Gideon Amir. | 6 |

Chemistry & Nanotechnology

| | |
|--|---|
| Ilana Karp :: Prof. Jordan Chill. | 8 |
| Aryeh Krischer :: Prof. David Zitoun. | 9 |

Psychology & Neuroscience

| | |
|--|----|
| Grace Aharon & Aviva Cantor :: Prof. Aron Weller. | 10 |
| Anna (Chaya) Apfel :: Prof. Ruth Feldman. | 11 |
| Aviva Cantor & Grace Aharon :: Prof. Aron Weller. | 12 |
| Shayna Goldstein :: Prof. David Anaki. | 13 |
| Rivka (Rebecca) Kurtz :: Prof. Eva Gilboa-Schechtman. | 14 |
| Rivka Salhanick :: Dr. Elana Zion Golumbic. | 15 |
| Madalyn Sarafzadeh :: Prof. Ronny Geva. | 16 |

Life Sciences: Ecology & Plant Science

| | |
|---|----|
| Sarah Gold :: Prof. Ilana Berman-Frank. | 17 |
| Yonatan Schwartz :: Dr. Gad Miller. | 18 |
| Eric Shalmon :: Prof. Lee Koren. | 19 |
| Tehilla Sollofe :: Prof. Ilana Berman-Frank. | 19 |

Life Sciences: Human Biology

| | |
|---|----|
| Yael Arshadnia :: Prof. Tammy Gershon. | 21 |
| Briana Friedman :: Prof. Ronald Goldstein. | 22 |
| Berel Gold :: Prof. Benny Motro. | 23 |
| Avital Habshush :: Prof. Ramy Don. | 24 |
| Miriam Pearl Klahr :: Prof. Binyamin Knisbacher. | 25 |
| Lily Ottensoser :: Prof. Haim Cohen. | 25 |
| Netanel Paley :: Dr. Galit Shohat-Ophir. | 26 |
| Michael Seleski :: Dr. Yossi Mandel. | 27 |
| Azriel Teitelbaum :: Dr. Ofir Hakim. | 29 |

Editors:
Grace Aharon
Aviva Cantor
Berel Gold
Shayna Goldstein
Ben Kaplan
Michael Seleski
Eric Shalmon

Layout & Design:
Tehilla Sollofe



Left to Right: Daniel Klovisky, Brian Snow, Andrew Katz, Ben Kaplan, Sara Palgon, & Tamar Felman

Signal Processing- Virtual Simulations of Geometrical Room Acoustics

Tamar Felman
Advised under Prof. Sharon Gannot and Mr. Pini Tandeitnik

One way to study the trajectory of a sound signal is to solve the acoustic wave equation that describes the given signal. Because a sound signal in space can have complicated shapes and properties, however, calculating a solution to the 3D acoustic wave equation has limited practical applicability in scenarios that involve irregular 3D domain boundary surfaces and mesh interiors, which are best described by non-Cartesian geometry. Using the wave equation to describe a sound signal in such a case would require the system to be broken into a large number of smaller elements, often a number too big to store in a computer's memory system. For example, a signal containing frequencies ranging from 100 Hz to 22000 Hz trans-

mitted in a $5 \times 5 \times 2 \text{ m}^3$ room would require the storage of about 1.85×10^9 mesh elements, which translates to over 20 GB of memory. This storage is required for the points that describe the system alone, and does not even include any calculations that will be done using those points.

Because describing a sound signal as a wave is complex, signal processing engineers often use a different method—ray acoustics. They consider a sound signal a ray along which its acoustic energy is transported. The propagation of a sound ray follows the same laws of reflection and refraction as light rays. This method of classification of a signal makes it simpler to determine its trajectory.

Bar Ilan University's speech and acoustics lab studies sound signals using the ray acoustics method explained above in order to develop more advanced methods of limiting sound reverberations and improving beamforming, filtering signal transmission and/or reception, in audio systems. The propagation

of signals is mapped out virtually using COMSOL, a multiphysics software that provides an interactive setup for modeling real-world acoustic scenarios.

COMSOL's ray acoustics interface computes the trajectories, phase, and intensity of acoustic rays, making ray acoustic calculations more manageable, practical, and require less computer memory than calculations of the solution to the acoustic wave equation would. The software simulates the transmission of a sound signal from source to sink, calculates the transfer function that relates the output signal(s) to the input signal(s), and then generates a mesh of the approximate solution. Although the solution is not exact, an approximate solution is sufficient at very high frequencies or very small wavelengths.

COMSOL Multiphysics software has the ability to simulate room acoustics as explained above when transmitted sound signals contain a single frequency. Accessing a COMSOL model through MATLAB and manipulating its variables from the MATLAB interface can extend the COMSOL ray acoustics interface's capabilities to plotting signals that contain multiple frequencies. Once expanded upon, the same technique can be used to simulate any acoustic room scenario and applied to the development of reverberation and beamforming technologies.

Observing Apoptosis by Means of Fluorescence Lifetime in Coated Gold Nanoparticles

Sara Palgon and Ben Kaplan

Advised under Prof. Rachela Popovtzer

Gold nanoparticles (GNPs) and gold nanorods (GNRs) have been shown to have a variety of diagnostic and therapeutic applications in the treatment of cancer. Gold nanoparticles are non-toxic and the high density of gold makes GNPs an excellent contrast agent for x-ray and CT scanning. Using GNPs as a contrast agent is particularly helpful in that it allows tumors to be imaged even when there is no large structure present. This allows very small tumors to be detected by CT, which can help medical professionals to detect and treat remaining cancerous cells after surgery.

Another possible application of GNPs to cancer diagnosis and therapy is using them to ascertain when cells undergo apoptosis¹. In our experiment, GNPs with a diameter of approximately 20 nm were fabricated. The success of the fabrication was confirmed by spectrophotometric methods. 90% of the surface of the GNPs was then coated with linkers attached to the glucose. Since cancerous cells have increased meta-

bolic activity, they take up the glucose-coated GNPs more readily than regular cells². 10% of the surface was coated with linkers which contained fluorescein at the end and which were conjugated with a caspase-sensitive peptide (DEVD).

The theory behind the experiment is that when fluorophores are within 40 nm of GNPs, the electric field of the GNP changes the fluorescent lifetime of the fluorophores. When the DEVD peptide is cleaved by caspase-3, the original fluorescent lifetime of the fluorophores is observed. Fluorescence-lifetime imaging microscopy (FLIM), which uses a laser to excite fluorescent particles, was used to observe changes in fluorescence lifetime (**Figure 1**).³ Unfortunately, neither the coated GNPs with caspase added to them nor coated GNPs which were examined in cells in which apoptosis was induced showed any change in fluorescence lifetime. Therefore, results are inconclusive at the time of this writing.

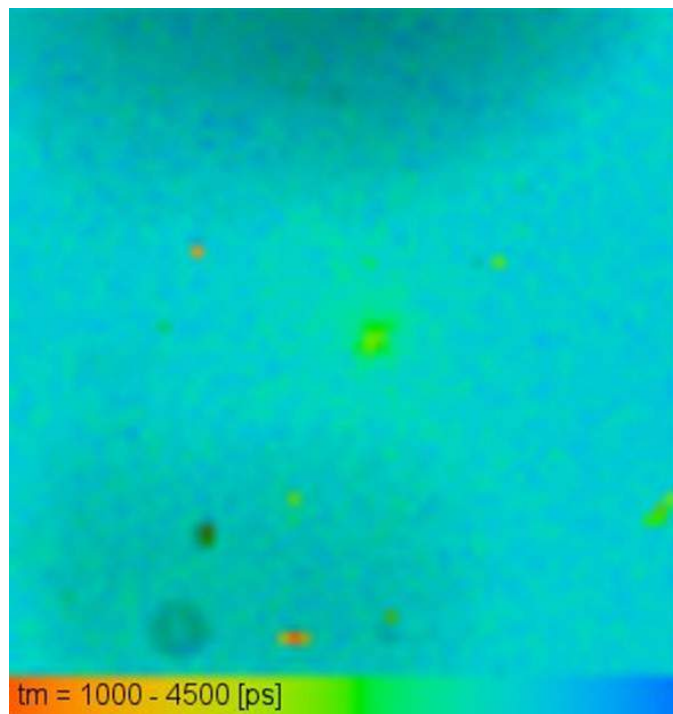


Figure 1. Sample of coated GNPs imaged using FLIM.

¹ Chen, W., Luo, G., Xu, X., Jia, H., Lei, Q., Han, K., & Zhang, X. (2014). Cancer-targeted functional gold nanoparticles for apoptosis induction and real-time imaging based on FRET. *Nanoscale*, *6*(16), 9531. doi:10.1039/c4nr02516d

² Motiei, M., Dreifuss, T., Betzer, O., Panet, H., Popovtzer, A., Santana, J., . . . Popovtzer, R. (2016). Differentiating Between Cancer and Inflammation: A Metabolic-Based Method for Functional Computed Tomography Imaging. *ACS Nano*, *10*(3), 3469-3477. doi:10.1021/acsnano.5b07576

³ Barnoy, E. A., Fixler, D., Popovtzer, R., Nayhoz, T., & Ray, K. (2015). An ultra-sensitive dual-mode imaging system using metal-enhanced fluorescence in solid phantoms. *Nano Res. Nano Research*, *8*(12), 3912-3921. doi:10.1007/s12274-015-0891-y

Detecting and Defining Tumors and their Margins through Gold Nanoparticle Luminescence Absorption Signatures

Andrew Katz

Advised under Dr. Dror Fixler

Accurate and early detection of malignant tumors is essential for effective cancer treatment. Computerized Axial Tomography scanning is currently the preferred method for detecting cancer, but it is far from a perfect process. The utilization of Gold Nanoparticles (GNPs) coated with Epidermal Growth Factor Receptors (EGFRs) is the latest method for early diagnosis and therapy treatment of cancer now being researched. GNPs are advantageous due to their inexpensive and non-invasive procedure, relative to CT scans, and for their desirable optical properties over other metals.

GNPs coated with EGFRs are ideal targeting and contrasting agents that can be used to search for and

detect tumors. The EGFR is a cell-surface receptor directly associated with human cancer. Tumor cells express over ten times the amount of EGFRs than normal cells (4×10^4 to 1×10^5 EGFR in a normal cell, and over 2×10^6 EGFR in a tumor cell). Therefore, ten times the amount of GNPs coated with EGFRs will collect in cancerous tissue than in healthy tissue. The quantity of EGFR that is present in the cells is directly correlated to the magnitude of GNP that will be absorbed by the cells. Since cancerous cells have a much higher count of EGFR than normal cells, higher levels of GNP absorption in an area of tissue likely indicate that that area is cancerous.

An experiment was conducted to test the tumor detecting capabilities of GNPs. Several locations on each of eight distinct salivary gland tissue samples were examined using hyper spectral imaging microscopy before and after GNP absorption. Luminescence absorbance spectras within the 450-950 nm wavelength range were obtained and evaluated at these sites to determine which areas contained high levels of GNP absorption. Although a negligible portion of the GNPs bind to healthy cells, the EGFR coating ensures that the GNPs target tumor cells and bind there in significant quantities.

After the absorbance spectras for a particular area of tissue were obtained before and after the addition of the GNPs, the two spectras were superimposed onto

one another by the computer software Nuance 2.0, and the GNP spectra (the only spectral difference between the two images) was isolated for analysis and evaluation.

Due to their specific optical properties, the gold nanoparticles used in the experiment have a defined peak at around 530 nanometers. A graph of the isolated spectra obtained after superimposing the before and after GNP images that have a high peak at the expected value of 530 nanometers indicates that a significant amount of GNP binded to those cells at that particular testing site and there is likely a tumor in that area (**Figure 1**).

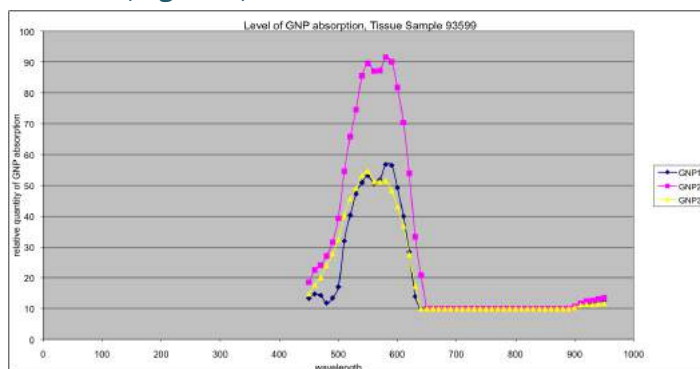


Figure 1. Spectra of GNP absorption isolated by subtracting the spectrums of the tissues with and without GNPs. The relatively high level of absorbed GNP coated with EGFR in the expected wavelength range indicates the likely presence of a tumor.

Over the course of the experiment, we attained high, medium, and low peaks of gold absorption measures, indicating which areas were likely cancerous, healthy, or bordering areas of tumors. The experiment highlighted the incredible potential for using gold nanoparticle technology to more precisely detect tumors and define tumor margins, which would yield more complete removal treatments in the future.

Pancakes, Hamiltonian Paths and Diameter

Daniel Klovsy

Advised under Prof. Yuval Roichman and Prof. Ron Adin in collaboration with Yuval H. Khachatryan

An important tool for the analysis of sorting algorithms is the study of permutations, which are linear orders on the letters $1, 2, \dots, n$ equipped with an adjacency relation. The *Cayley graph* on the symmetric group S_n is the graph where the set of vertices consists of all permutations on n letters and edges determined by a chosen generating set. My research is focused on the study of Cayley graphs on the symmetric

group with respect to distinguished sets of generators, and some quotients. One important parameter is the minimum number of successive applications of generators that is needed in order to arrive at any permutation from any other permutation. This is the diameter of the corresponding graph.

Initially we chose the generating set of the following action(s) on the permutation: taking a prefix of any length and flipping the order, i.e. 14583276 becomes 85413276 by taking a prefix of length 4. This determines the Cayley graph on S_n with prefix reversals as the generating set. We analyzed the algebraic structure, in particular relations and cycles, in this graph. We found that the diameter question had been posed as the "pancake problem" [3] [6] and was addressed by Bill Gates [5] and others. Linear bounds on the diameter are known, see [2].

A double flip is a simultaneous reversal of a prefix and of its complement (the suffix). Taking only double flips as generators, we proved that the resulting graph is disconnected. In this case the graph decomposes into $((n-1)!)/2$ connected components, each of which is isomorphic to the Turan graph $T(2n,2)$ - a symmetric complete bipartite graph of order $2n$.

A Hamiltonian path in a graph passes through every vertex exactly once. Drawing the vertices as those of a regular n -gon, we consider the Hamiltonian paths that do not cross themselves. Two Hamiltonian paths are adjacent if they differ in exactly two edges. The resulting graph on all non-crossing Hamiltonian paths in the complete graph of order n was introduced in [7]. The diameter was evaluated in [1].

A permutation in S_n can be viewed as a directed Hamiltonian path in the complete graph of size n , with the only vertex with in-degree 0 as the first term in the permutation, the next vertex adjacent to it as the second term, and so on. Non-crossing Hamiltonian paths correspond to so-called *arc permutations*. This leads to a new interpretation of a result of Elizalde and Roichman [4] as an evaluation of the diameter of graphs on directed non-crossing Hamiltonian paths with respect to a different adjacency relation. Motivated by this observation, we consider the graph on arc permutations generated by prefix reversals, suffix reversals, and double flips. Translated to Hamiltonian paths, these actions consist of deleting an edge and adding another, switching directions of edges to create a new Hamiltonian path. My focus here is on enumerating vertices and their degrees and identifying central vertices and other properties of the graph in order to establish the radius and diameter. Solution

of this diameter problem has significant ramifications in complexity and network analysis.

- [1] J.-M. Chang and R.-Y. Wu, On the diameter of geometric path graphs of points in convex position, *Inform. Process. Letters* 109(8) (2009), pp. 409--413.
- [2] B. Chitturi et. al., *An $(18/11)n$ Upper Bound for Sorting by Prefix Reversals*, *Theoretical Computer Science* 410(36) (2009), pp. 3372-3390.
- [3] H. Dweighter (pseudonym of J.E. Goodman), *Elementary Problems*, *American Mathematical Monthly* 82(1975), p. 1010
- [4] S. Elizalde and Y. Roichman, *Arc Permutations*, *Journal of Algebraic Combinatorics* 39(2) (2014), pp. 301-334.
- [5] W.H. Gates and C.H. Papadimitrou, *Bounds for Sorting by Prefix Reversal*, *Discrete Mathematics* 27 (1979), pp. 47-57.
- [6] Online Encyclopedia of Integer Sequences, A058986
- [7] E. Rivera-Campo and V. Urrutia-Galicia, Hamilton cycles in the path graph of a set of points in convex position, *Comput. Geom.* 18 (2001), pp. 65--72.

The Probabilistic Theory Underlying Interacting Particle Systems

Brian Snow

Advised under Dr. Gideon Amir

When simulating an interacting particle system, there are two fundamental types of models one can use. In one model, the deterministic model, there is an assumed certainty in all internal aspects of the model. By inputting various parameters into the model, one will be able to see the various results associated with the different sets of parameters.

In contrast to a deterministic model, a stochastic model has a random element included within the model. When simulating a stochastic process, one will not get one result, rather one will get a distribution which will represent all the possibilities and the probability with which each possibility will occur.

With the guidance of Dr. Gideon Amir, I analyzed a number of stochastic processes. These included the contact process, the population competition model, and random walks. The contact process can represent the spread of an infection or the growth of a population. For example, at a given time, the state of $[0, 0]$ on the grid is infected while all the other points on the grid are healthy. In the contact process, each infected point on the grid becomes healthy at a constant rate. However, the rate of infection is based on an exponential random variable. The probability that a given point will become infected either increases or decreases depending on how many of its neighboring points are infected.

The significance of this process is that it is modeled using an exponential random variable which is an

example of a Markov process. A Markov process is memoryless which means that no past state in the process or model has any impact on the future. The future state is totally determined based on the current state and the various random and deterministic parameters which were put into the model.

One can further complicate the contact process model with the population competition model. In a population competition model, one studies what happens not only when there is one population growing on the grid but also if there are two populations competing for space. One can investigate how the two populations will interact with each other. Depending on various parameters that one can set up, the populations may either both grow infinitely as time goes to infinity, or one of the populations may end up dying out.

In addition to studying these models, I also analyzed random walks in various dimensions. In a simple model of a random walk, there is a point on the grid which at each discrete time unit will move one step in any direction based on a random variable. In one or two dimensions, it can be shown through simulations and mathematical proofs that the point will likely

return to 0 (or $[0, 0]$) as time goes to infinity (**Figure 1**). However, in a three dimensional random walk, the percentage chance that the point will return to its starting place decreases significantly.

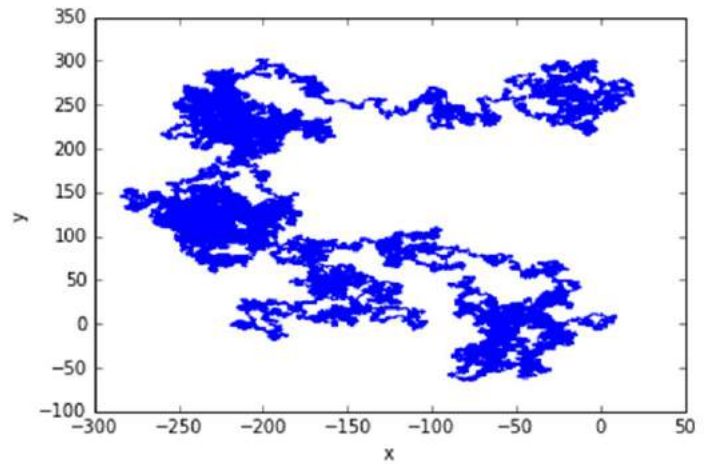


Figure 1. Path of a 2D random walk of 100,000 steps in discrete time based on a simulation created by the author. Notice that despite the length of the simulation, the point has stayed relatively close to the point $[0, 0]$. This highlights the idea that a 2D random walk will almost certainly return to its starting point as the random walk continues to infinity.



Left to Right: Aryeh Krischer & Ilana Karp

Studying Hui1 and KcsA through NMR Spectroscopy

Ilana Karp

Advised under Prof. Jordan Chill and PhD student Netanel Mendelman

K⁺ channels in cell membranes allow K⁺ ions to translocate through the cell membrane. Several toxins (such as the ShK toxin from the sea anemone) were found to inhibit K⁺ channels and are being used for therapeutic and scientific applications. Therefore, inhibiting specific K⁺ channels is of great importance. One specific toxin, ShK, was found to inhibit the hominine voltage gated K⁺ channel (Kv1.3). ShK, however, does not bind to the model K⁺ channel KcsA. Scientists in Brandeis University used the amino acid sequence of ShK to manufacture a toxin that can inhibit KcsA. The result is a new toxin called Hui1.

What this study intends to investigate is what makes Hui1 bind to KcsA while ShK cannot. In order to understand this we must study the binding of Hui1 to KcsA. The first step is to express the toxin in *E. coli*.

However, due to the disulfide-disulfide interactions in Hui1, there is a high probability that Hui1 will fold incorrectly while being expressed in bacteria.

In order to correct this problem, the toxin must first be unfolded then refolded in the correct structure. Hui1 is expressed with a his-tag and a TEV cleavage sequence. First, Urea and DTT are used for unfolding Hui1. The his-tag is used for binding Hui1 to a nickel beads column. Washing the column with Urea and DTT unfolds the protein. Gradually removing Urea and DTT enables Hui1 to refold in the correct structure (with the right disulfide bridges). Elution of Hui1 from the column is obtained by washing the column with a high concentration of imidazole buffer. Next, TEV, a protease enzyme, is added to Hui1 solution thus detaching the his-tag from the correctly folded toxin. Lastly, the toxin solution is lyophilized and the toxin is dissolved in another buffer solution for NMR measurements.

In the NMR, each peak represents an amino acid in the protein sequence (except proline). The NMR peaks

of Hui1 as shown in **Figure 1**, allow us to study the structure and dynamics of the toxin. Future studies will allow understanding the nature of the binding between Hui1 and KcsA. This will give us a clue about how other toxins bind to different K⁺ channels.

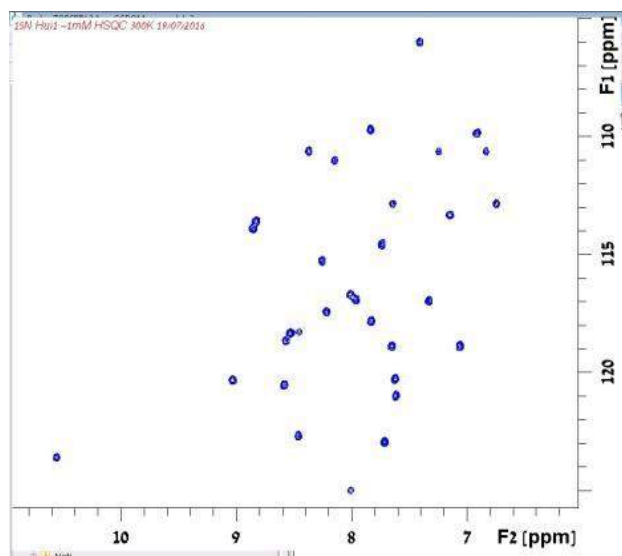


Figure 1. NMR spectrum of Hui1

Hydrogen Sensing

Aryeh Krischer

Advised under Prof. David Zitoun and PhD student Guy Rahamim

Sensing hydrogen – detecting and measuring the concentration of hydrogen in an environment – presents an important challenge from both a diagnostic and a safety-oriented perspective. Hydrogen is highly explosive and leaks easily, so a sensor able to measure hydrogen concentration could detect leaks and significantly improve safety. From a diagnostic perspective, a hydrogen sensor would enable laboratory and industrial settings that use hydrogen to measure parameters and ensure processes are proceeding smoothly.

Most commercially available sensors, and indeed,

most sensors that have been studied, rely on the reactivity of hydrogen in the presence of certain metals. Chief among these reactive metals is palladium, which acts as a “sponge” and readily absorbs incredibly large volumes of hydrogen. As palladium absorbs hydrogen it becomes PdH (palladium hydride), with vastly different properties from the original palladium. Of chief importance among these changes is a marked decrease in electric and thermal conductance. It is upon this change that sensors are typically based; the measured resistance of a sample of palladium will increase proportionally to the amount of PdH present which in turn increases proportionally to the concentration of hydrogen in the surrounding environment¹.

We rely on the same measurement techniques but with two major changes, the method of fabrication and the introduction of nickel. Nickel is known to provide reversibility to the hydrogen-absorption reaction of palladium, so we use a nickel-palladium alloy to fabricate our sensors.

Our method of fabrication relies on a technique developed in the lab of Hagai Shpaisman. In short, laser heating of a colloidal suspension of nanoparticles causes deposition along the path of the laser. We use this technique, in partnership with the Shpaisman lab, to deposit the palladium-nickel alloy to fabricate our sensors.

After initial testing, it was found that the sensor exhibited a near-instantaneous response in the presence of hydrogen and a recovery time (return to ground state) of approximately 20 seconds, which is a fantastic time frame.

With this proof-of-concept complete, we look forward to optimizing the sensor fabrication in terms of production of materials used and ease of fabrication. Furthermore, we look forward to new deposition methods and new materials to test for improving reactivity and reversibility.

¹ Hubert T., Boon-Brett L., Black G., Banach U. (2011). Hydrogen Sensors – A Review. *Sensors and Actuators B: Chemical*, 157(2), 329-352. doi: 10.1016/j.snb.2011.04.070



Left to Right: Shayna Goldstein, Rivka Kurtz, Rivka Salhanick, Chaya Apfel, Madalyn Sarafzadeh, Aviva Cantor, & Grace Aharon

Effect of L-arginine on the Appetitive Behavior of Hungry Rats

Grace Aharon and Aviva Cantor

Advised under Prof. Aron Weller and M.Sc. student Kayla Rapps

Obesity is one of the most serious issues plaguing the global community today, posing far-reaching consequences to public health. Obesity results from overconsumption and reduced energy expenditure, which induce an imbalance in homeostatic energy. A deeper understanding of energy balance regulation, therefore, is critical to treating and preventing obesity.

Nitric Oxide (NO) is a naturally-released gaseous molecule found in most living organisms and spanning a wide variety of functions in the body, including vasodilation and food regulation. L-arginine, a dietary amino acid, is the substrate for synthesis of NO in the body and in the brain. Recent studies in the marine slug *Aplysia* and in mammals indicate that NO, under conditions of satiation and low motivation to eat, is a weak inhibitor of feeding. In contrast, research in *Aplysia* further shows that under conditions of high motivation to eat, NO increases appetitive behavior.

There have not yet been studies investigating the consumatory impact of L-arginine in mammals under conditions of high motivation to eat.

The objective of this study is to investigate the effect of NO on feeding in adult male rats under conditions of high motivation to eat. Based on research in *Aplysia*, we hypothesize that animals that have been injected with L-arginine, a substance that increases the production of NO, will show increased appetitive behavior, or at least will not show decreased feeding, compared to controls.

To ensure the condition of high motivation to eat, the animals were made to be hungry at the start of the experiment by providing them with only 60% of their normal chow consumption the previous night. At the start of the experiment, the hungry animals received an intra-peritoneal injection of either L-arginine in saline (N=4) or a vehicle treatment (saline, N=4). The dosage administered to the animals was 150 mg/kg. After a 5-minute recovery period, the animals were returned to their individual experimental cages with free access to 20 grams of chow. Their appetitive behavior was observed and recorded for 1 hour. Appetitive behavior was defined as approaching, sniffing,

and/or eating the chow.

The results of the study show that the mean number of meals in the control group was slightly less than that of the experimental L-arginine group. On average, the control group exceeded the L-arginine experimental group in duration of animals' first meals, time spent eating, total time of appetitive behavior, total grams of chow consumed, bout length, and bout size. However, when the data from the study were analyzed using several two-tailed independent t-tests, $p < .05$, it is evident that the differences in feeding between the control group and the experimental L-arginine group are not significant. Note the relatively small N per group. The trend in the data seems to indicate that the administration of L-arginine and increased production of NO reduces appetitive behavior in hungry rats. Further experimentation on additional subjects is necessary to ascertain whether this trend of L-arginine-induced decreased feeding in hungry animals is indicative of a significant effect. It is clear, however, that administration of this dose of L-arginine under conditions of high motivation to eat does not increase appetitive behavior in adult male rats.

The Long-term Effects of Kangaroo Care on the Development of Premature Infants

Anna (Chaya) Apfel

Advised under Prof. Ruth Feldman and PhD student Adi Yaniv

Previous studies have demonstrated that premature birth can have deleterious effects on child development such as lower academic, cognitive and emotional abilities¹. Additionally, past studies have found lower amounts of white matter in the brains of premature births and have suggested that this decrease may lead to many of the cognitive dysfunctions found in children born prematurely².

A common intervention to combat these adverse effects is skin-to-skin contact, or kangaroo care. Though previous studies have researched the immediate positive effects of kangaroo care, as of now no studies have looked at the long-term effects kangaroo care has on the future development of the child. Researching this is important in that it will further the present knowledge on kangaroo care and possibly instigate the conception of future interventions to reduce the negative effects of premature birth.

Our current longitudinal study is researching the long-term effects kangaroo care has on the development of premature babies. Participants were 146 premature babies born in Israeli hospitals between December 1996 and September 1998. The participants were randomly distributed into two groups of 73 each; one group received kangaroo care while the other received customary NICU treatment. Participants were visited seven times throughout their childhood and were given a series of tests with which to assess different cognitive abilities. The most recent study showed that receiving kangaroo care can have positive effects later in life; participants at age ten showed a decreased response to stress, superior cognitive control and autonomic functioning, and a more mutual mother-child rapport³.

Participants are presently being visited again at age 18 to evaluate the effects in adults who have had neonatal kangaroo care. Using questionnaires, saliva samples, in-person interactions, and magnetic imaging methods such as functional MRI and diffusion tensor imaging, researchers are studying and comparing brain activity, anxiety, depression, attachment, empathy, and synchrony in the two participant groups. Additionally, this study will combine both the behavioral and neurological tests to see if kangaroo care has an effect on either.

It is hypothesized based on past research that the kangaroo care group will have significantly lower anxiety and depression levels and higher attachment, empathy and synchrony scores as compared to the control group. Additionally, it is hypothesized that the brain activity in the kangaroo group will show higher axial diffusion and lower radial diffusion levels, leading to the conclusion that the kangaroo care group has a positive effect on white matter integrity.

Though there are no significant results as of yet as researchers are still collecting and analyzing the data, the data that has been analyzed seems promising in support of the hypotheses.

¹ Allen, M. C. (2008). Neurodevelopmental outcomes of preterm infants [Abstract]. *Current Opinion in Neurology*, 21(2), 123-128. doi:10.1097/wco.0b013e3282f88bb4; Campbell, C., Horlin, C., Reid, C., McMichael, J., Forrest, L., Brydges, C., . . . Anderson, M. (2015). How do you think she feels? Vulnerability in empathy and the role of attention in school-aged children born extremely preterm. *British Journal of Developmental Psychology*, 33(3), 312-323. doi:10.1111/bjdp.12091; Richards, J. L., Chapple-Mcgruder, T., Williams, B. L., & Kramer, M. R. (2015). Does neighborhood deprivation modify the effect of preterm birth on children's first grade academic performance? *Social Science & Medicine*, 132, 122-131. doi:10.1016/j.socscimed.2015.03.032

²De Kieviet, J. F., Zoetebier, L., Elburg, R. M., Vermeulen, R. J., & Oosterlaan, J. (2012). Brain development of very preterm and very low-birthweight children in childhood and adolescence: A meta-

analysis. *Developmental Medicine & Child Neurology*, 54(4), 313-323. doi:10.1111/j.1469-8749.2011.04216.x; Hack, M. (2006). Young adult outcomes of very-low-birth-weight children. *Seminars in Fetal & Neonatal Medicine*, 11(2), 127-37. doi:10.1016/j.siny.2005.11.007
³Feldman, R., Rosenthal, Z., & Eidelman, A. I. (2014). Maternal-Preterm Skin-to-Skin Contact Enhances Child Physiologic Organization and Cognitive Control Across the First 10 Years of Life. *Biological Psychiatry*, 75(1), 56-64. doi:10.1016/j.biopsych.2013.08.012

The Effect of Trait Binge Eating on the Conflict between Immediate Pleasure and Delayed Aversive Consequence: A Rat Eating Behavioral Model

Aviva Cantor and Grace Aharon

Advised under Prof. Aron Weller and MA candidate Lital Moshe

Decision making research often looks at a number of personality traits and conflict variables that influence the choices we make. One important conflict examined is the choice to act in a way that is immediately rewarding but has delayed negative consequences. Our lab aims to identify the biological basis and neural mechanisms that underlie such decisions. To do so, we use a behavioral model, in which rats are presented with the choice to consume highly palatable foods (PF) that are associated with delayed digestive discomfort. We chose to examine the impact of “trait binge eating” on the preference for PF under potentially aversive conditions.

Binge eating (BE) is a maladaptive eating pattern in which one rapidly consumes a larger than normal amount of food, and highly palatable foods are salient stimuli for binge eating. In our study, we examined whether the level of PF preference for Oreo cookies, accessible for a limited duration (4 hours, every 2-3 days), is affected by the expectation of a delayed negative digestive consequence (lactose-induced lower abdominal discomfort). Adult rats typically experience digestive discomfort as a result of lactose ingestion due to low levels of intestinal lactase activity. Because the negative digestive response does not immediately follow the intake of lactose, we attempted to produce a learned association of the abdominal discomfort with the PF, which the rats received in the study around the same time the abdominal discomfort appeared.

Binge eating prone (BEP) and binge eating resistant (BER) PF eating patterns in rats is an established paradigm that allows us to differentiate between individuals with and without “trait BE.” In the first stage of

our study, 46 adult female Wistar rats were characterized and categorized into the two trait BE groups, BEP and BER, based on a series of 3 tests in which they were given Vanilla Ensure Plus, a nutritional substitute (and PF), to consume. Rats were ranked according to amount of Ensure consumed in comparison to body weight on days 2 and 3, and rats that consumed more than the median Ensure consumption were categorized as BEP.

We hypothesized that there would be a difference in PF consumption (binge size) between BEP and BER groups while tolerating the lactose-induced lower abdominal discomfort. Lactose ingestion, as compared with glucose ingestion, would be associated with a decrease in the consumption of PF, especially in the BER group. BEP lactose rats were expected to consume as much PF as the BEP glucose group, regardless of the lactose-induced lower abdominal discomfort. The amount consumed by the BEP lactose group was also expected to be greater than the amount consumed by the BER lactose group.

During the second stage of the experiment, both BEP and BER rats were conditioned to anticipate the PF. To accomplish this, rats were given a solution of glucose mixed with Ensure, which upon finishing or after 60 minutes had passed, were then presented with Oreo cookies, the PF.

In the next stage of the experiment, BEP and BER rats were randomly assigned to either the lactose (experimental) or glucose (control) condition. At the beginning of the test, each animal was presented with a dish containing the sugar and Ensure solution in an empty cage. After finishing the Ensure solution, or after 60 minutes with the Ensure had passed, rats were placed in a regular test cage with standard rat food (Chow) and Oreos (the PF). Chow and PF measurements were taken after 2 hours and 4 hours to determine how much each rat ate. There were 3 test days. Preliminary results indicated that BEP lactose rats consumed significantly more Oreo vs. chow/body weight than the BER lactose rats ($p=.02$). Specifically, on the third test, BER rats that received lactose consumed PF equivalent to 1.88% of their body weight, while BEP rats that received lactose consumed PF equivalent to 2.82% of their body weight during the 4 hour test period (**Figure 1**).

The final test in this experiment was performed a week after the third lactose v. glucose test and aimed to identify conditioned memory effects in the BEP and BER rats. Researchers hoped to determine if the rats

retained a memory of the negative digestive consequence they had associated with the PF and whether it would affect their choice to consume more PF. This test included only the control glucose condition. Preliminary results point to a memory effect in the BER rats. BER rats that had previously received lactose consumed only PF equivalent to 1.05% of their body weight at 2 hours, while BEP rats that had previously received lactose consumed PF equivalent to 2.15% of their body weight after 2 hours. This indicates that the BER rats retained the impression that they would receive lower abdominal discomfort from the PF and thus ate less compared to the BEP group. BEP rats showed less memory for the food-induced discomfort, which may be related to their BE trait.

Before the animals were sacrificed at the conclusion of the experiment, they were exposed to the smell of Oreos and given a glucose + Ensure mixture to promote anticipation of the PF. Brain and blood samples were then collected from these rats and will be analyzed for neurochemical correlates related to anticipatory behaviors and biological correlates of anxiety and emotional behaviors.

Individual differences in lactase activity among the rats may be a confounding variable in this study, and future studies may want to assess the lactase activity of each individual rat before lactose consumption. Additionally, BEP and BER rats may differ in their level of pain sensitivity, and researchers may choose to examine the number of pain receptors in the periaqueductal gray (PAG) to investigate this difference.

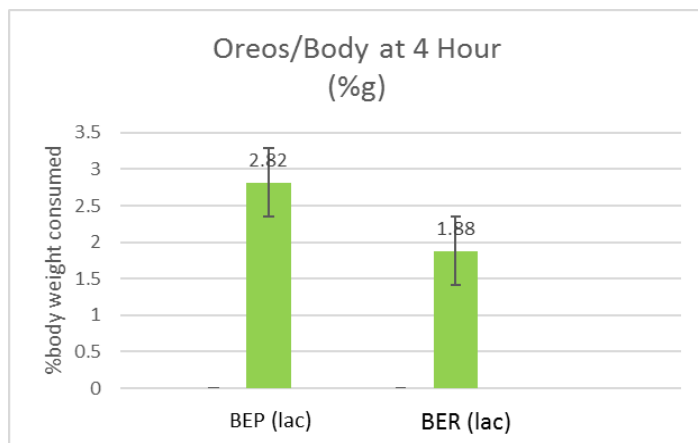


Figure 1. Oreos Consumed/Total Body Weight at 4 Hours on Third trial.

Recognition of Familiar Faces is Influenced by Both Amount of Exposure and Semantic Information

Shayna Goldstein

Advised under Dr. David Anaki and MA candidate Yishai Deitscher

This experiment investigated the mechanisms people use to recognize familiar faces. Possible reasons for remembering a face include exposure (how many times the face has been seen before) and knowing semantic information about the face, which may strengthen the memory trace. This study differs from other experiments in that it examines how these factors independently effect facial recognition, and that the study takes place over a longer period of time, one week, rather than just one session.

Faces were familiarized to participants over the course of the six day experiment using E-Prime software. The exposure frequency of individual faces was manipulated so each face was shown either twice or four times per session. Additionally, half of the faces were shown with name and profession as semantic information. Thus, there were four conditions: no semantic information with two exposures; no semantic information with four exposures; with semantic information with two exposures; with semantic information with four exposures. Thirty-two faces were taught on days 1-4, followed by a review test. In the test, participants were shown each face and then asked whether a name was given and whether a profession was given. Each question included five choices: the information was not given, the information was given but the participant does not remember, and three choices each of names or professions, respective to the question. On the third and fourth days there was a rehearsal session after the test where faces from previous days were shown again. The fifth day was a rehearsal of all 128 of the previously learned faces. On the sixth day, participants took a test on all the faces, plus new faces. For each face, they were asked if the face was old or new, and they were given the same questions about the semantic information as on the other days. Event Related Potentials (ERP) were measured using the BioSemi EEG system to measure brain activity during the final test.

Behavioral results of accuracy on the final test show that both frequency and semantic information are important main effects for remembering faces (**Figure 1**). No interaction effect was seen, showing that each factor operates independently. Preliminary

analysis of ERP results (Figure 2) indicates differences in the posterior P1, posterior N170, and posterior N250. There seems to be an effect on brain activity from becoming accustomed to a face, which can be seen in the weaker P1 peak in response to seeing faces from the semantic information and four exposures condition. This indicates that less attention needs to be given to a more frequently exposed face than to a less familiar face. A similar effect was found at the N170, which responds to facial processing, but its significance is not determined because the peak to peak difference was the same. The N170 seemed to respond more strongly to faces with semantic information than faces without semantic information. Additionally, the N250, which has been implicated in detailed processing of faces, shows the strongest peak in the semantic information with four exposures condition. There is an interaction effect seen at all of these peaks, where the combination of semantic information and exposure four times has a stronger effect than any of the other three conditions. A more thorough statistical analysis is necessary before conclusive differences can be determined in either the behavioral or ERP results.

This experiment was conducted in Hebrew. A pilot study of an English version of the experiment was performed on 5 participants, with the hopes of being able to expand the study to a larger population, and to add fMRI data to future studies.

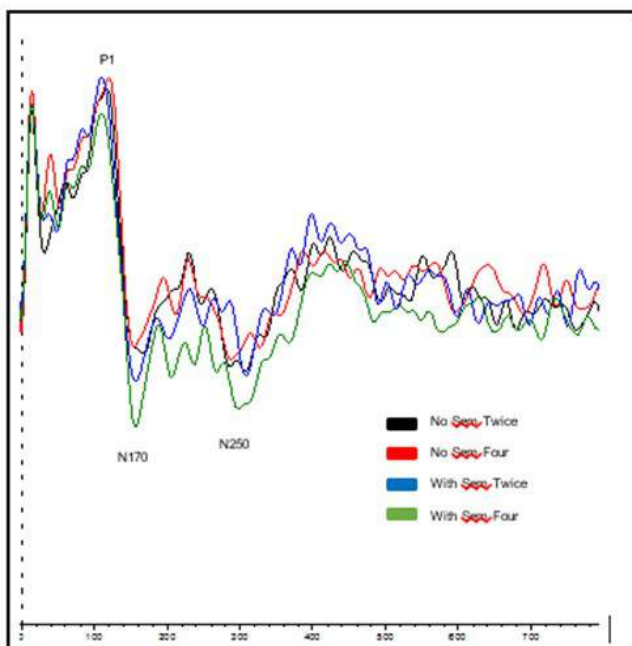


Figure 2. Effects of exposure and semantic information of P1, N170, and N250 amplitude.

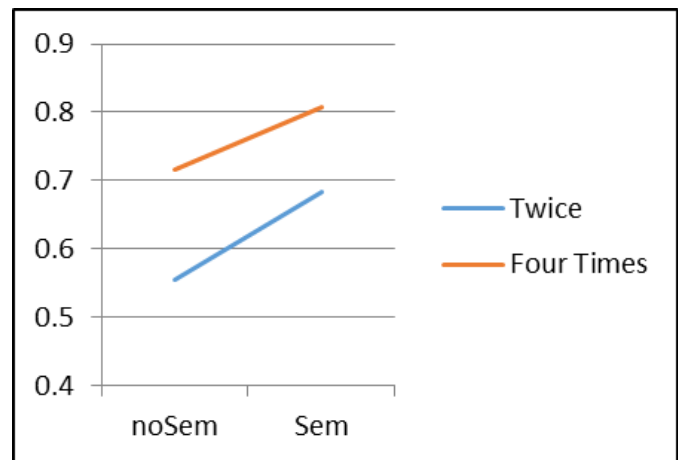


Figure 1. Effects of exposure and semantic information on recognition memory of faces.

Anger and Facial Processing

Rivka Kurtz

Advised under Prof. Eva Gilboa-Schechtman and PhD student Hadar Keshet

Faces are gold mines of information. On a simple level, they assist us in recognizing people and their emotions, but faces also serve as important stimuli for social decision-making and judging personality traits (Olivola, Funk, & Todorov, 2014). By monitoring people's responses to the different kinds of facial cues, we can learn important information about the way individuals respond differently to various facial expressions. Facial cues can be present in two distinct ways: either as emotional facial expressions, or as actual facial characteristics and structure.

The Gilboa-Schechtman lab focuses on a combination of facial processing and social anxiety disorder. Socially anxious individuals are hypersensitive to being evaluated in social settings and tend to pick up on subtler social cues than individuals without social anxiety. One of the lab's recent experiments aimed to discern whether socially anxious individuals are more sensitive to all facial cues, or specifically to dominant looking faces. During this experiment, the participants were assessed using the Dominance Perception Task (DPT), a computerized task that presents pairs of dominant faces. The participants were asked to choose the face in each pair that looked more dominant to them. The task was also modified to present faces with varying degrees of trustworthiness in order to ascertain whether socially anxious individuals are more sensitive to those kinds of faces. The final results indicated that individuals high in social anxiety are indeed more accurate at pointing out faces that

are more dominant, and not faces that are less trustworthy.

In addition to this line of research, another series of studies has examined how individuals tend to infer character traits based solely on facial appearance, as opposed to emotional expressions. For example, one study showed how people's judgments of politicians' characters based on their faces can predict which politician will attain office (Olivola et al., 2014). These kinds of judgments, or so-called "face biases," can be applied to clinical topics as well. Although the lab studies social anxiety disorder, I was interested in applying this research to understanding how individuals high in trait anger (an increased propensity for anger) process dominant looking faces. Previous research has shown that individuals prone to anger and aggression tend to utilize what is called a hostile attributional bias. This means that they interpret ambiguous situations and stimuli as hostile or threatening. In terms of processing facial emotions, research has shown that individuals high in trait anger are more attuned to angry faces and anger-related stimuli (Van Honk, Tuiten, de Haan, de Hout, & Stam, 2001) (Parrott, Zeichner, & Evces, 2005). Based on these findings and the research concerning face biases, I planned an experiment to investigate whether individuals high in trait anger are more sensitive to specific kinds of facial traits. The design would have participants first complete the Buss-Perry aggression inventory to receive a ranking as either high or low in aggression and anger. Participants would then be presented with the same DPT task that the lab used to assess the relationship between social anxiety disorder and dominance perception.

The implications for this research are important and exciting, as anger is one of the basic emotions and has an impact on interpersonal relationships as well as personal wellbeing (Owen, 2011). Should the results indicate that individuals high in trait anger are in fact more sensitive to dominant looking faces than people with low trait anger, these findings would add to the increasing research on face biases and could help influence therapeutic approaches.

Virtual Reality LipSync Unity Project

Rivka Salhanick

Advised under Dr. Elana Zion Golumbic

Traditionally, neurological experiments have used discrete stimuli such as pictures, sounds, light signals,

etc. to study neural responses. Although these stimuli help to create a very well controlled setting for an experiment, the setting remains an artificial, unnatural setting, very different from our own busy and noisy environments. In a natural setting, we encounter many stimuli simultaneously. Thus said, the Golumbic lab focuses on studying neural mechanisms in more natural settings that are closer to these real-life situations. This is difficult to achieve because a completely natural setting cannot easily be controlled.

Common stimuli used in experiments to maintain a near natural setting are audiovisual filmed clips, which can be shown on a computer screen to participants. However, this mechanism is difficult to manipulate and does not lend itself to multiple circumstances. My lab has focused on using advanced technological tools, such as virtual reality, to create natural, real-life stimuli that can be easily manipulated and configured according to the experimenter's goals. Specifically, we want to be able to manipulate these stimuli to study how eye contact, body position, voice volume, distractions, and other factors affect brain processes. We can also track a subject's eye movement, to monitor where the subject is focusing his attention throughout the course of the study.



Figure 1. Artemis the avatar alongside the WAV file with phoneme markers

My project throughout the summer was to create part of these virtual reality stimuli through the use of a 3D development environment program, Unity 5.3. With this program, I lip synced audio files to an animated avatar, "teaching" the avatar to move his mouth in sync with the audio clip by attaching Hebrew phoneme markers to a series of fifty WAV sound files (**Figure 1**). Phonemes are distinct units of sound that distinguish one word from another, for example the *o*, *r* (throat reish), *ch* (throat chet), and *s* (samech or sin). In Unity, each of these phonemes were matched

with particular mouth movements, for example the *o* phoneme will make the avatar have rounded, open lips and mid-mouth to the left and right (Figure 2), the *ah* phoneme will make the avatar have open, wide lips (Figure 3), and the *m* phoneme will make the avatar have closed lips and slightly puffed cheeks (Figure 4). Now, when played back, the avatar can speak in sync with the audio file.



Figures 2 & 3. Avatar “saying” *o* (right) and “saying” *ah* (left)



Figures 4. Avatar “saying” *m*

Examining Joint Attention Behaviors in Infants using the Early Social Communication Scale

Madalyn Sarafzadeh

Advised under Prof. Ronny Geva and students Anastasya Olkin and Jessica Schreiber

Joint Attention (JA) involves the ability for two people to collectively attend to an object. Joint Attention is understood to be associated with language development skills as well as positive affect behaviors, such as smiling. Joint Attention measures behaviors such as eye gazing on objects, alternation of gaze between objects and another person, eye contact, pointing, as well as gesture communication.

Studies have suggested that development of joint attention

may contribute to skills that provide children with the foundations to acquire language. Previous studies found that the more time infants spent in joint engagement with another party, such as a mother, the more vocabulary words they knew. Development of joint attention may help explain individual differences in how children acquire language. Children with Autism spectrum disorder (ASD) have been reported to have deficits in joint attention skills and relatedly, deficits in language development.

In addition to language, previous research suggests associations between positive affect behaviors, such as smiling, and joint attention in children. Researchers have looked at two different types of smiling patterns during joint attention behaviors, reactive smiles as well as anticipatory smiles. Reactive smiles occur when a child first smiles at another person and then gazes at an object while still smiling. In an anticipatory smile, a child gazes at an object, smiles, and then smiles at another person. Studies have concluded that anticipatory smiles are related to peer communication abilities.

As joint attention has been suggested to contribute to social developmental skills such as language development and positive affect, I hypothesized that there would be significant correlations found between joint attention behaviors and positive affect social interactions, as well as development of language.

The current study looks at early social communication behaviors, such as joint attention in infants aged 9 months. Participants are observed using the Early Social Communication Scale (ESCS), an interactive task in which the experimenter provides different toys to the child. Interactions are later evaluated for various social communication factors, including eye contact with the tester while holding a toy, displaying anticipatory smiles, displaying reactive smiles, following the gaze of the tester, initiating requests for a toy and engaging in turn-taking games. Participants are also observed using an additional computerized gaze contingent eye-tracking task known as the Speech task. In this task, participants are assigned videos of a woman speaking to them in Hebrew and in “gibberish.” The video was activated based on where the child was looking, and measures included preference for Hebrew or “gibberish” videos.

Results indicated significant correlations between anticipatory smiles and child-initiated joint attention (IJA). Additionally, increased IJA was significantly related to time of looking at the Hebrew speaker over the video with “gibberish,” nonsense language. This result was still significant when holding age as a covariate.

By better understanding relationships between joint attention and development of language and behaviors of positive affect in infants, we can analyze more closely specific communication skills in preverbal infants. We can monitor preferences for language and social interaction at a younger age and their growth of development. The relationships can help us learn about significance of joint attention in early social communication behaviors.



Left to Right: Sarah Gold, Tehilla Sollofe, Eric Shalmon, & Yonatan Schwartz

Aquatic Microbial Ecology and Oceanography

Sarah Gold

Advised under Prof. Ilana Berman Frank, Dr. Hila Elifantz, PhD student Itai Landau, and MSc student Tslil Bar

Nitrogen fixation is a process in which bacteria fix dinitrogen (N_2) to produce a more usable form of nitrogen, such as ammonia (NH_3). This biological process is an important source of usable nitrogen (N) for the oceanic and terrestrial systems that are responsible for stimulating production and growth of microbial communities and the entire ecosystem at large. ("Dinitrogen fixation in aphotic oxygenated marine environments", Berman-Frank, (2013) A significant amount of nitrogen fixation is attributed to the filamentous cyanobacteria *Trichodesmium*. (Segregation of Nitrogen Fixation and Oxygenic Photosynthesis in the Marine Cyanobacterium *Trichodesmium*, Berman-Frank (2001) Our objective was to see if *nifH*, a protein specializing in nitrogen fixation in various cyanobacteria, is instrumental in *Trichodesmium*'s diazotrophy. The techniques we used included DNA extraction and PCR. Then the amplified products were

separated on agarose gel and photographed (Figure 1). Our results were inconclusive and further cloning and purification of the DNA samples are necessary.

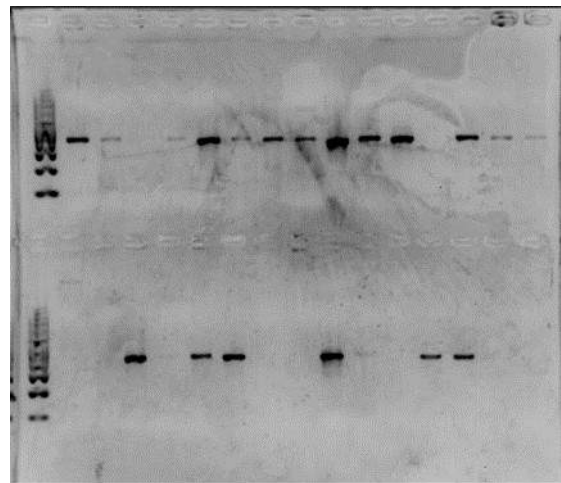


Figure 1. Photograph of gel electrophoresis of *Trichodesmium* gene sequence

The East Mediterranean Sea is a nutrient-poor area which is exposed to environmental and anthropogenic impacts; therefore, it is important to monitor this

ecosystem. Phytoplankton have an important role in the marine food web and are the producers of the oxygen supply of the ocean and of Earth's atmosphere. The lab had previously been working on determining seasonal depths distribution of phytoplankton and bacterioplankton community at certain locations using the CytoSub, a machine specializing in flow cytometry, and bench top FACs (Fluorescent Activated Cytometer). In addition, we also wanted to characterize the phytoplankton and bacterioplankton community using chlorophyll and phylogenetic affiliation.

We collected sea-water samples from various depths and enriched them with a stable nitrogen isotope. Future plans of researchers include estimating new and export production of organic material, specifically of N₂, in the Gulf of Aqaba. Further research will be done to identify the nitrogen fixing bacteria present and quantify them using the CytoSub and the FIRE fluorometer, which is used to measure chlorophyll fluorescence in photosynthetic organisms.

Improving Pollen Tolerance to Heat Stress (HS) By Using Pollen-Specific HS-Induced Promoters

Yonatan Schwartz

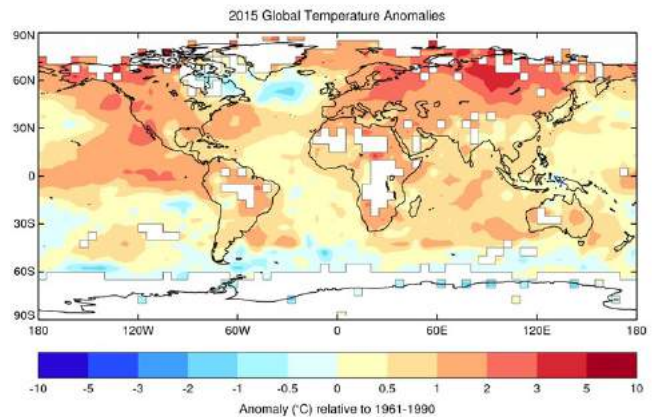
Advised under Dr. Gad Miller and PhD student Gilad Luria

Extreme climatic stresses on a plant impair its ability to carry out photosynthesis, limit growth, and cause the destruction of reproductive organs. The male organs in particular are the most susceptible tissues of the plant to environmental factors. Even a short period of mild stress could irreversibly impair their functionality.

According to the US National Oceanic and Atmospheric Administration, 2015 was the warmest year to have been recorded since the official records began in 1880 (Figure 1). Studies continue to show that higher temperatures are expected in the future. NASA's Goddard Institute for Space Studies (GISS) in New York reported that each of the first six months of 2016 set a record as the warmest month globally in the official records. Because the world's food supply is mainly derived from the products of plant sexual reproduction, it is of utmost importance to study pollen biology (the biology of the male gametophyte of the plant) in the hopes of creating stress-tolerant plants.

Our research focuses on promoters which activate pollen-specific genes during heat stress. Our goal is to identify which promoters become most active and attach these promoters to other genes which help the

pollen become more capable of tolerating heat stress.



<https://www.wmo.int/media/content/2015-hottest-year-record>

Figure 1. A map of the global temperature fluctuations (in Celsius) for the year 2015 relative to the temperatures recorded from 1961 to 1990.

The model organism the lab works with is *Arabidopsis thaliana*, a plant known for its small genome and relatively short life cycle. Our lab has recently conducted an RNA sequencing assay to compare the transcriptional footprint of normal plants with those of plants which were recently affected by heat stress. The results led us to certain genes whose expression was strikingly up-regulated in pollen during stress. Based on the results, our current aim is to confirm that the promoters of those genes are indeed pollen-specific and induced uniquely by stress.

The project focused on creating transgenic *Arabidopsis* plants containing these promoters. In order to execute this procedure, we amplified two promoters from the plant's genome and transferred them to a plasmid-bearing GUS (Figure 2). The GUS reporter system is composed of a reporter gene (enzyme) which, when activated by a promoter, forms a visible, blue precipitant. We hypothesize that if the promoter is indeed more active during stress, only the pollen of the GUS-containing plants will turn blue. In order to successfully create a generation of plants with this exact plasmid, we carried out an *Agrobacterium*-mediated floral transformation. *Agrobacterium* is a genus of soil bacteria which has the ability to cause tumors in plants. They are the only known case in nature of a living organism capable of transferring DNA to another organism's genome. Hence, *Agrobacteria* are widely used in plant molecular biology. Once we successfully transferred the plasmids to the *Agrobacteria*, we introduced flowering *Arabidopsis* plants to the bacteria in order for the plasmid to be fused

with the plant's genome. After several antibiotic-based selections and self-fertilization, independent homozygous transgenic lines will hopefully be generated. These lines will serve as an example of how pollen grains sense and react to heat and, therefore, as a pivotal tool for improving crops yields.

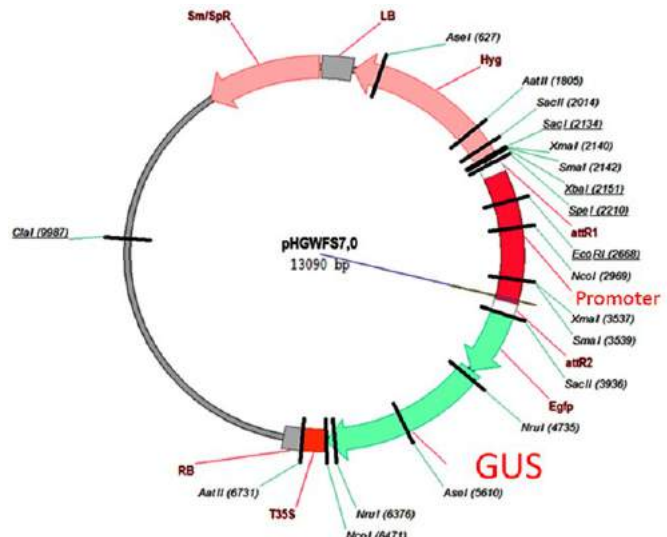


Figure 2. A map of the plasmid pHGWFS7,0 containing the promoter we selected combined to GUS.

Roughness in Hyrax Vocalizations: An Honest Signal

Eric Shalmon

Advised under Prof. Lee Koren and PhD student Yishai Weissman

Animal vocalizations can include reliable qualities that indicate an individual's traits (e.g. social status or size), based on the source-filter theory, which proposes that voice production is shaped by the characteristics of the vocal tract, and Zahavi's handicap principle, which hypothesizes that reliable or truthful signals of any sort (including vocalizations) must cost something to the signaler such that one with less of a certain trait can not mimic the signal. One such property is the "roughness" of an animal's voice - quantified by the voice's jitter, the variation in frequency of sound waves, and shimmer, the variation in amplitude of sound waves. Commonly, when an animal is excited or aroused, its voice becomes rougher. To produce that rough sound, the animal must expend extra energy (i.e. the cost of the honest signal.)

Male rock hyraxes, *Procavia Capensis*, produce a complex song, composed of a number of elements, one of which is a snort. The snorts are the rough part of their song and the roughness and length of snort are

hypothesized to represent the hyrax's age/weight and aggressiveness/social status. Over 100 playback experiments were performed in the Ein Gedi Nature Reserve on the local hyrax populations. Only when four hyraxes were spotted together was an experiment performed because it could be assured that a singing male was in the vicinity, if not one of the four. It was recorded whether a male hyrax responded to the playback with his own song or not.

For the playbacks, four natural songs were used. For each song, there were four manipulations and two controls - altogether 24 different playback tracks. The snorts in each song were manipulated to be long or short and smooth or rough. Experiments on the same group of hyraxes were only performed 30 minutes apart to prevent habituation to the synthetic songs. Furthermore, whenever there was a disturbance, such as a passing fox or an alarm call from a hyrax pup, five minutes were allowed to pass before performing the experiment, so that it could be assured that any song was in response to the playback and not in response to the disturbance. After the playback song completed, a two and a half minute gap was given for a response because in natural settings, hyraxes reply to a song as late as two and a half minutes after the songs completion.

Statistically, it was found that hyraxes responded more frequently to songs with shorter, smoother snorts rather than the longer, rougher snorts, as expected. The rougher, longer snorts dissuaded other hyraxes from responding because they purportedly represented a more aggressive, larger hyrax. It was hypothesized that less hyraxes responded to songs with long, rough snorts because they couldn't produce a song of the same length and compete with another hyrax of such caliber; to other hyraxes, the roughness was an honest signal of the singing hyrax's aggressiveness and high social dominance rank.

Trichodesmium Efficacy in Oligotrophic Waters

Tehilla Sollofe

Advised under Prof. Ilana Berman Frank, PhD students Yael Tsubari and Etai Landau

Fixation of atmospheric dinitrogen introduces a bioavailable form of nitrogen into nitrogen-poor surface waters of the ocean providing an essential component for organisms at the base of aquatic food webs. Blooms of *Trichodesmium*, a planktonic marine cyanobacterium, are responsible for 25 to 50% of marine

and global nitrogen cycling and therefore essential for promoting marine life growth. The unique habitat resultant of *Trichodesmium* blooms lead to a complex assemblage of microzooplankton, where nutrient transformation and exchange can take place¹. *Trichodesmium* can exist as single trichomes or colonies, which determines the efficiency of the associated microbe community².

Oligotrophic bodies of water, such as the Gulf of Aqaba, lack inorganic nutrients. Diazotrophic (nitrogen fixing) organisms are especially sensitive to iron (Fe^-) and phosphate (PO_4^-) concentrations at surface level. Therefore, the effect of Fe^- and PO_4^- limitation on *Trichodesmium* colony formation was investigated. We subjected two samples of *Trichodesmium* to Fe^- deplete media and compared cell count and colony formation to a control sample (non depletion). It was found that Fe^- deficiency has a high influence on colony formation after 48 hours (Figure 1). The same was done with PO_4^- , and the results suggest that while PO_4^- deficiency induces colony formation, Fe^- deficiency affects colony formation much more rapidly (48 hours versus 6 days).

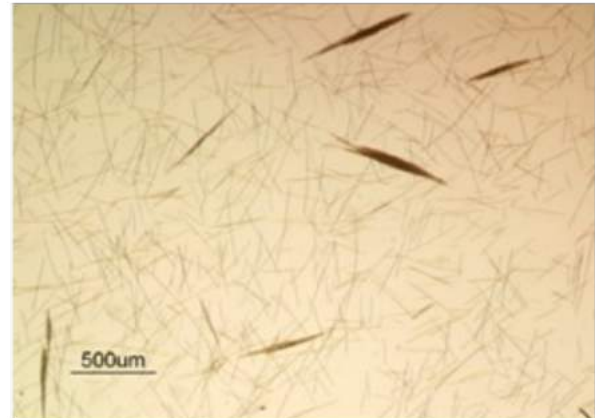


Figure 1. Trichomes and colonies in Fe depleted media

Another objective was to study the unique environment of the Gulf of Aqaba and predict possible repercussions of environmental change. As part of this ongoing study, sea-water samples from various depths were profiled for chemical and physical properties and then tested for nitrogen and carbon fixation rates. As a follow-up to that project, the samples will be analyzed for diazotroph identification.

¹Sheridan, C., D. Steinberg, and G. Kling. 2002. The microbial and metazoan community associated with colonies of *Trichodesmium* spp.: a quantitative survey. *Journal of Plankton Research* 24:913-922.

²Capone, D. G., J. P. Zehr, H. W. Paerl, B. Bergman, and E. J. Carpenter. 1997. *Trichodesmium*, a globally significant marine cyanobacterium. *Science* 276:1221-1229.



Back Row Left to Right: Berel Gold, Azriel Teitelbaum, Michael Seleski, & Netanel Paley
 Front Row Left to Right: Lily Ottensoser, Yael Arshadnia, Avital Habshush, & Briana Friedman

(Not Pictured: Miriam Pearl Klahr)

The Relationship Between TRF2 and Various Basal Transcription Factors in Transcription Regulation

Yael Arshadnia

Advised under Prof. Tammy Gershon and PhD student Adi Kedmi

The core promoter is a regulatory element in the transcription process of the eukaryotic cell that varies both in structure and function, depending on the gene. Transcription can be initiated in one of two ways: focused and dispersed. Focused initiation occurs in a localized region of the core promoter, either at a single nucleotide or in a small group of nucleotides, whereas dispersed initiation involves a few weaker transcription start sites that are found within a 50-100-nucleotide range. Although simpler organisms usually undergo focused transcription initiation and most vertebrate cells undergo dispersed transcription initiation, a small yet important group of vertebrate genes still undergo focused transcription

initiation. The structure of the focused core promoter varies significantly depending on the absence and/or presence of specific sequence motifs like the TATA box, DPE (Downstream core Promoter Element) etc. (Figure 1).

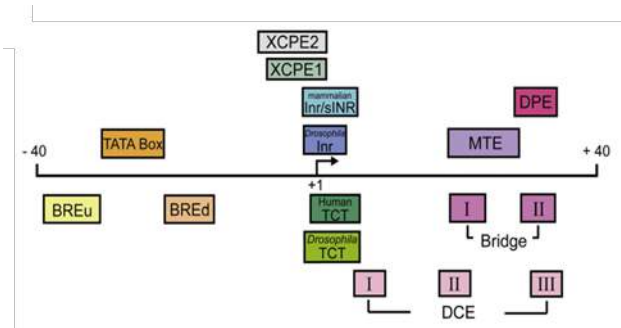


Figure 1. Schematic illustration of the most common core promoter elements found in focused promoters.

In order to facilitate gene expression, components of the basal transcription machinery recognize and bind to the core promoter, and subsequently recruit RNA Polymerase II to the transcription site in order to facilitate gene expression. These basal transcription

components are called TFIIA, TFIIB, TFIID, TFIIE, TFIIIF, and TFIIH (Figure 2).

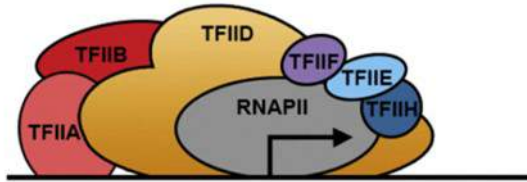


Figure 2. The assembly of the basal transcription machinery on the core promoter (arrow represents core promoter)

The first basal transcription factor that is responsible for recognizing and binding to the core promoter is TFIID, a complex of TBP (TATA Binding Protein) and various TAFs (TBP Associated Factors). TBP activates TATA box dependent transcription and represses DPE dependent transcription, thus regulating TATA dependent versus DPE dependent transcription. The TAFs that surround TBP aid in regulation of the transcription initiation and gene expression (Figure 3).

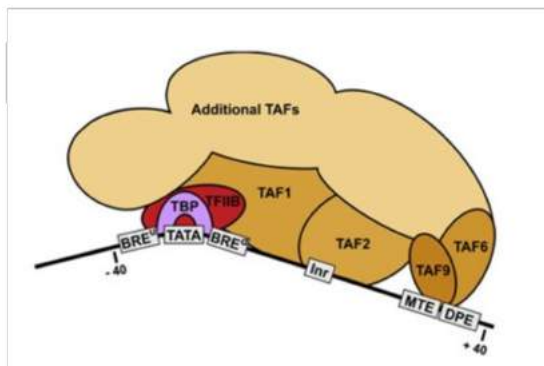


Figure 3. Zooming in on the DNA-binding PIC components (TFIIB and TFIID).

Transcription is regulated by assorted core promoter elements and basal transcription machinery. A good example of such assortment is the existence of three types of TBP-related factors (TRFs): TRF1, TRF2, and TRF3.

The family of TRF proteins shows high homology to the C terminal core domain of TBP. The structure of the TBP C terminal domain allows it to interact with the TATA-box. TBP, TRF1 and TRF3 can activate TATA box dependent transcription. However, of the three types of TRF (TRF 1, 2, and 3) TRF2 is the least similar to TBP and thus cannot interact with the TATA-box. Since TRF2 lacks the amino acid construct that is required for TATA box binding, it therefore does not bind to the TATA box in the core promoter. Instead, it

activates DPE and other types of TATA-less promoter dependent transcription as opposed to TATA box dependent transcription, and is thus involved in the regulation of different genes from TBP. Consequently, there is reason to believe that like TBP, TRF2 warrants its own complex, comprising of an entirely unique composition of TAFs and other transcription factors.

The focus of this study is to determine which other transcription factors work in tandem with TRF2 and to explore the possibility of unique TRF2 gene expression (i.e. genes that cannot otherwise be expressed in the TBP/TFIID complex). Through the process of immunoprecipitation, it was thus far determined that TRF2 works with TAF1, TAF4, and TAF6. Over the course of several weeks, TAF1, TAF4, and TAF6 genes as well as PET15b, PET 29, and pFastBac plasmid vectors were cloned and sequenced by PCR. The long-term goal is to study gene expression regulation, specifically the expression of the various TAF proteins in conjunction with TRF2 in bacterial cells. This will be done by inserting each of the TAF proteins into each of the vectors and then transferring the vector-insert complex into bacterial cells, which will in turn produce proteins. These proteins will be extracted, purified, and subjected to *in vitro* transcription. The products of this *in vitro* transcription - RNA which code for various proteins - will shed light on which of the other proteins are indeed necessary in TRF2 initiated transcription.

Establishing a New Technique for the Generation of Human Peripheral Sensory Neurons for the Study of the Varicella Zoster Virus

Briana Friedman

Advised under Prof. Ronald Goldstein

VZV (Varicella Zoster Virus or human herpesvirus 3, HHV-3) is a pathogenic human alpha herpesvirus that causes varicella (chicken pox). Primary infection begins with inhalation and subsequent systemic delivery to the dermis of the skin where it causes itchy, inflamed blisters. Infection also takes place in the peripheral nervous system and establishes a long period of latency in the trigeminal, autonomic and dorsal root ganglia of the peripheral nervous system. After a variable period of time, usually decades, the virus can reactivate, either spontaneously or due to a variety of factors, including increased age and immunosuppression. The reactivated virus causes herpes zoster

(shingles), a disease characterized by extremely painful vesicular skin eruptions and frequently complicated by acute pain, diverse neurological sequelae, vision problems, and long lasting post-herpetic neuralgia. The events surrounding VZV's latent state and reactivation are difficult to study due to a lack of model systems for latency and reactivation because of the human specificity of the virus. There is no widely-used in vivo small animal model in which reactivation can be experimentally induced.

As such, there is a need to create an experimental model for VZV latency and reactivation. Since the virus is human-specific, it is necessary to obtain human neurons. Professor Ron Goldstein's lab has been creating nerve cells for many years using embryonic stem cells. Recently, his lab established a model for latency and reactivation for VZV using these hESC-derived neurons. However, one issue with the model is that it uses a mixture of CNS and PNS neurons. Even cadaveric sensory neurons are not ideal for use as they have limited availability and have difficulty surviving in culture. The goal of the project that I worked on was to produce peripheral sensory neurons utilizing the transcription factors Ngn1, Ngn2, and Brn3a, based on a recent publication.

E-coli bacteria were transformed through heat shock, causing an uptake of lentiviral plasmids containing the specific neuronal transcription factors, which were obtained courtesy of Dr. Kristin K. Baldwin of The Scripps Institute at University of California San Diego¹. The bacteria were plated on agar and incubated overnight to increase the plasmid amount before harvesting. The plasmid was extracted and its concentration was measured using a nanodrop spectrophotometer. After extraction, plasmids were cut with restriction enzymes and run in a gel to verify that the correct plasmids were amplified. The plasmids were then utilized to create lentivirus, a retrovirus that is derived from HIV and used as a vector to introduce foreign genes into cells. The neurogenic plasmids were transfected along with plasmids containing lentiviral packaging proteins into murine 293 cells. A control virus constitutively expressing GFP was also generated to follow visually production of lentivirus. After allowing for production of the virus for 48-72 hours, the supernatant was collected and the lentivirus was concentrated. The GFP lentivirus was tested for its ability to infect human dermal fibroblasts and 293 cells. Initial results indicate that lentivirus was generated, but at a very low yield. The neurogenic lentivirus will ultimately be used to infect embryonic

stem cells in the hope that this will cause peripheral neuronal differentiation, allowing study of VZV in cells that are infected in actual varicella disease.

¹ Blanchard, J.W., Eade, K.T., Szűcs, A., Sardo, V.L., Tsunemoto, R. K., Williams, D., ... Baldwin, K.K. (2014) Selective Conversion of fibroblasts into peripheral sensory neurons. *Nature Neuroscience*, 18(1), 25-35. doi: 10.1038/nn.3887

BG-1 Interaction with BU-2

Berel Gold

Advised under Dr. Benny Motro and MSc student Grace Swickley

Disclaimer: The names of the relevant proteins in this study were changed in order to protect the findings of this study.

Little is currently known about cell protein BG-1, but evidence suggests that full knockout of BG-1 in the embryo is fatal. Further evidence indicates that BG-1 may localize to both the nucleus and the cytoplasm, suggesting that BG-1 has roles in both. Evidence from our lab suggests that BG-1 binds with protein BIU-2, a protein whose function is not currently known, in the cell. This study intends to uncover which part of the protein BG-1 binds with BIU-2.

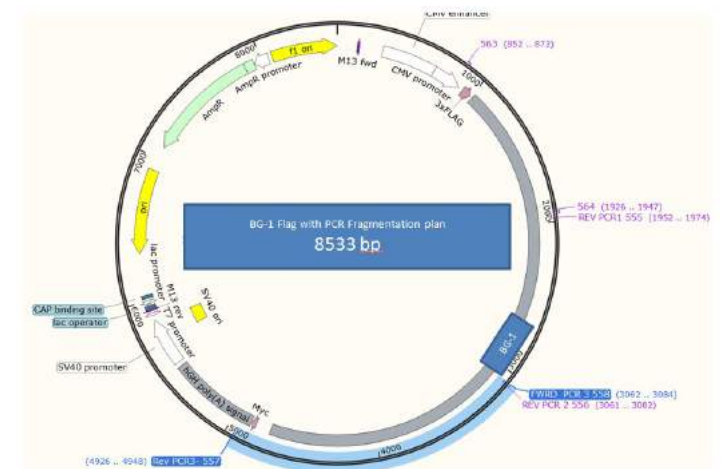


Figure 1. Fragmentation Plan

To do this, we cloned the gene which codes for BG-1 into 4 different parts using a variety of primers. We then incorporated each part into a cell plasmid and tested where each fragment bound. Unfortunately, only one fragment was successfully cloned, which will be subsequently referred as "frag3." Figure 1 shows the fragmentation plan for frag3. Since this is the only DNA fragment we were able to amplify, it is the only fragment's protein product we tested to bind to BU-2.

After cloning the DNA fragment in the PCR, the PCR fragment was cut with restriction enzymes BamH-I and Hind-III. The fragment was ligated into a backbone plasmid, using the vector as a positive control. After ligation, the newly created plasmids were transfected into new bacterial cultures. Three cultures were made: the insert, the vector and a control with the now transfected plasmid. After growing these cultures overnight, the colonies were transferred to an LB solution (with AMP, an antibiotic, added) to be amplified. The colonies were sent to sequencing in order to confirm that the plasmid with frag3 was fully incorporated. The colonies were then purified to obtain the proteins. A co-immunoprecipitation was run in order to show the relevant protein to protein interactions. Each protein has a specific marker which binds to the protein and can be identified by precipitating an antibody to that specific marker. The marker used to BG-1 is FLAG and the marker for BIU-2 is HA. The extract with a FLAG antibody was co-immunoprecipitated, and it bound with any FLAG tagged protein (i.e. BG-1 fused to flag). Figure 2 shows that the FLAG antibody precipitated BG-1-FLAG and FRAG3-BG1-FLAG, and these proteins co-precipitated with BIU-2 which suggests that the protein product of frag3 binds with BU-2 in the cell.

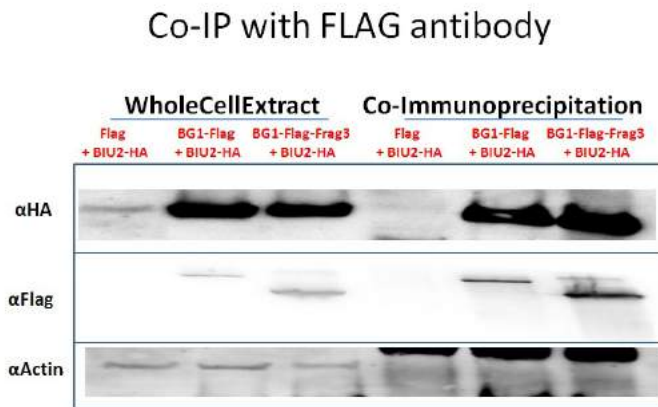


Figure 2. Co-immunoprecipitation Results

MEIG1 and its Dimeric Form

Avital Habshush

Advised under Prof. Jeremy (Ramy) Don, Dr. Leah Levin, and MSc student Eliezer Shai

The Meig1 gene is a highly evolutionarily conserved gene found in many different types of organisms: from single-celled organisms to humans. Meig1 is expressed abundantly during spermatogenesis, especially during the meiotic stage. Professor Don's lab

observed that knockout mice (mice that do not contain the Meig1 gene) are unable to produce mature spermatozoa, and there is an increase in apoptosis. Delayed kinetics of spermatogenesis have also been observed in knockout mice. Therefore it can be concluded that Meig1 is integral to spermiogenesis and meiosis.

Further investigation into Meig1 has shown that MEIG1 protein is integral in DNA repair. Professor Don's lab observed delays in DNA repair in meiosis and spermiogenesis in knockout mice. Since the abundant DNA breaks cannot be corrected, cells undergo apoptosis.

The MEIG1 protein's average weight ranges from 12-18 kDa. The Don lab also observed bands of 31-32 kDa under non-reducing conditions, while in reducing conditions, these bands cannot be seen. The Don lab postulated that the 31-32 kDa band comes from a dimeric form of MEIG1 due to one cysteine at position 75 in the amino acid chain. A disulfide bond between the cysteines of two monomeric MEIG1 proteins forms the MEIG1 dimer.

It has been observed that only the dimeric form of MEIG1 enters the nucleus as part of DNA repair. An experiment was done where fibroblasts were exposed to DNA damaging environments. An increased expression of the dimeric form of MEIG1 in the nucleus was observed. When MEIG1 was silenced, DNA repair slowed. When MEIG1 was given externally, the DNA damage response resumed. The Don lab hypothesized that MEIG1 must exist in the dimeric form in the nucleus in order to carry out DNA damage response.

In order to prove that MEIG1 contains disulfide bonds, MEIG1 mouse protein was expressed in bacteria and tagged with histidine. The protein underwent DNA analysis through PCR, mini prep plasmid purification, and gel electrophoresis. It was determined that the bacteria contained the plasmid.

The next step in the procedure was protein extraction and analysis. More bacteria were grown and underwent sonication. After extracting the proteins, the total amount of protein underwent affinity purification with nickel resins. The nickel resins bound to the histidine tag on MEIG1, separating it from the rest of the proteins. Afterwards imidazole, which has structural similarities to histidine was used to eliminate the MEIG1 histidine tagged protein. The proteins were then analyzed with a Western blot and transfer.

A stained band appeared at about 30 kDa in the western gel the size of the dimeric MEIG1 protein. However, the band only appeared in the sample containing the total proteins sonicated from the bacteria. The band did not appear in the purified solution containing only the MEIG1 protein.

After running the experiment with the control bacteria, the bacteria was mutated and analyzed. Mutation of DNA was done through PCR of bacteria by using specific primers, Meig1_t223g R and Meig1_t223g F. The mutation replaced the cysteine group responsible for the disulfide bond of MEIG1 and its dimeric form.

After DNA and protein analysis, no bands were observed. This could be due to the older resins used for the affinity purification. Other issues may have been due to compromised quality of certain reagents and antibodies. The Don lab hopes to repeat the experiment and further investigate the structure of MEIG1.

Uncovering Mobile Element Insertions in Lab Mouse Strains Using MELT

Miriam Pearl Klahr

Advised under Prof. Binyamin Knisbacher and Erez Levanon

Transposable elements are DNA sequences that play a unique role in the genome. These elements replicate using a copy and paste mechanism that sometimes results in evolutionary changes. Identifying these Mobile Element Insertions (MEIs) can play a crucial role in understanding the genetic variation within a species, including mutations that often lead to fatal diseases. In the lab, understanding variation between lab mouse strains is crucial for reliability and reproducibility of experiments used with this model organism. MELT, a java based software package, is one tool capable of accomplishing the task of identifying mobile elements. By comparing whole genome sequencing data to the respective organism's reference genome, it can identify novel MEIs. MELT characterizes the MEIs and reports which genes they disrupt. While MELT has been tested with human, chimpanzee, and dog genomes, it has never been used with those of mice.

In this study, we used MELT to analyze whole genome sequencing obtained from 13 mouse strains regularly used in labs, and identified MEIs of an active mouse transposable element (IAP). Then we used the R programming language and Excel for descriptive statis-

tics and biological interpretation. To analyze the genes disrupted by MEIs we used tools such as STRING and GREAT, which enabled to identify biological pathways enriched in MEIs. To further analyze the genes of interest harboring MEIs, we used the NCBI gene database to scrutinize the possible implications of the MEIs on organismal function.

The Effect of SIRT6 on Lipid Metabolism

Lily Ottensoser

Advised under Prof. Haim Cohen and PhD student Shoshana Naiman

As scientists continue to make breakthroughs in modern science and in medicine, there have been many advances in extending human lifespan. However, with increased longevity, there has been a rise in age-related metabolic diseases such as hypertension and obesity. It has been proven that a calorie-restricted diet can slow aging and extend lifespan, though the mechanism by which this occurs is not fully understood. Professor Haim Cohen's lab focuses on the metabolic pathways that work to increase longevity and their relationship to the sirtuin family, a group of NAD⁺ dependent deacylases that have been shown to play an important role in the regulation of extended lifespan and healthy aging.

In previous experiments, Professor Cohen's lab has shown that SIRT6 is involved in regulating diet and metabolic pathways. When caloric intake was restricted in mice, SIRT6 expression increased. Mice deficient in SIRT6 had metabolic deficiencies, died prematurely, and displayed aging-related phenotypes. Mice genetically altered to overexpress SIRT6 were found to have an extended lifespan when compared to normal mice, and they also appeared to have substantial improvement in their health as they aged. Research from Professor Cohen's lab has also implicated SIRT6 in regulating hepatic fat metabolism and beta oxidation, the process in which fatty acids are broken down during starvation. When both wild type mice and mice overexpressing SIRT6 were treated with WY 14,643, a specific PPAR activator that activates beta oxidation, it was found that the SIRT6 mice had altered beta oxidation genes, showing that SIRT6 interacts with PPAR in order to regulate beta oxidation.

Based on the findings that SIRT6 works with PPAR to play a role in metabolic pathways, we decided to further investigate the role of SIRT6 in the mechanism of

beta oxidation. We cloned PPAR from mouse cDNA in order to engineer cells to overexpress the PPAR gene. Upon successful cloning and amplification of this gene, we genetically modified Hepa-16 liver cells via transfection to overexpress SIRT6, PPAR, and a PPAR-specific promoter (PPRE element).

To investigate whether the deacetylase catalytic activity of SIRT6 is required for its regulation of PPAR activity, we treated cells with WY 14,643 and measured PPAR-mediated gene expression in the treated cells via qPCR. We found that cells that overexpressed SIRT6 showed greater beta oxidation gene activation when compared to cells without SIRT6 or with a mutant catalytically dead SIRT6.

After seeing such a strong effect of SIRT6 on beta oxidation, we sought to investigate the mechanism by which SIRT6 regulates PPAR genes. We transformed cells with the normal or mutant SIRT6, and also transformed cells with PPRE fused to a luciferase gene in liver cells. We then utilized the dual luciferase assay to examine the activity of the PPRE in cells with wild type SIRT6, mutant SIRT6, and knockout SIRT6 in the presence or absence of PPAR (Figure 1). We expected to see greater PPRE activity in the presence of PPAR and SIRT6 than in the presence of PPAR alone. However, the results show that PPRE activity was greater in the presence of PPAR alone. SIRT6 appeared to inhibit the expression of the PPAR promoter-luciferase construct, indicating a novel mechanism for the activation of WY-dependent genes that is not PPRE dependent. More experiments are required for further analysis, but these results could shed light on a yet unknown mechanism used to burn fat.

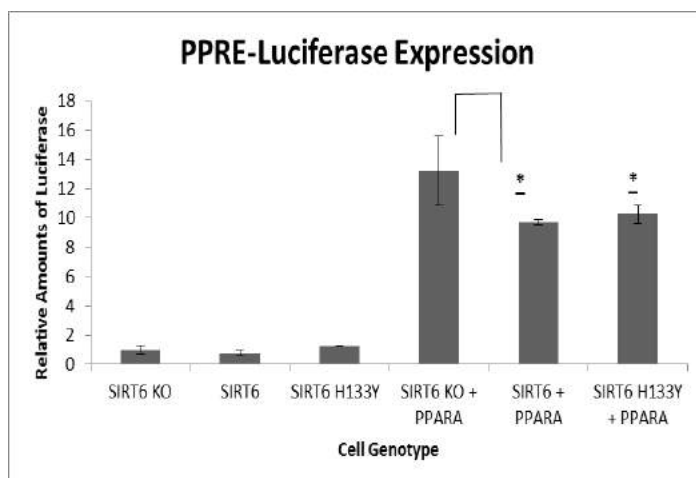


Figure 1. PPRE activity increases in the presence of PPAR. In the presence of PPAR and either SIRT6 or mutant SIRT6, PPRE activity increases but is somewhat inhibited.

These results and continued research hold promise in using SIRT6 as a drug target to prevent metabolic diseases and to promote healthy aging.

The Molecular Genetics of a Depression-Like State in *Drosophila*

Netanel Paley

Advised under Dr. Galit Shohat-Ophir and MSc student Assa Bentzur

The fruit fly, *Drosophila melanogaster*, has become an invaluable subject for neurobiological studies of behavior. Its intermediately sized neural network strikes an optimal balance between simplicity and sophistication, consisting of straightforward circuits that modulate a wide range of complex behaviors. The dual goal of Dr. Galit Shohat-Ophir's research is to investigate how these circuits operate as well as to identify the genes that control their operation. To this end, the massive body of research on the *Drosophila* genome together with recent technological advances in molecular genetics allow for facile genetic manipulation of neural pathways and even individual neurons with spatial and temporal specificity. Upon application of such methods and observation of fly behavior in controlled settings, we can propose and test neurogenetic mechanisms that underlie specific behavioral modalities. Conventional laboratory techniques such as real-time PCR and Western blotting allow us to quantitate the differential gene expression that governs these mechanisms, in terms of both RNA transcription and translation.

Our project was based on a 2013 study that demonstrates a correlation in *Drosophila* between uncontrollable heat stress and a motivational state known as learned helplessness. Learned helplessness is defined as an animal's passive reaction to a negative environmental condition or stimulus that cannot be ameliorated by an active behavior. When the animal learns that the stimulus is beyond its control, it will decrease its overall level of activity in addition to its specific efforts to overcome the unfavorable condition. In mammals, this state is associated with poor learning, sleep and feeding disorders, and immunodeficiency, and is thus proposed as an animal model of depression. In the aforementioned study, one group of flies was exposed to one-second heat shocks when they stopped walking, but could stop the heat by resuming walking. A second group was also exposed to one-second heat shocks upon resting, but could *not* stop the heat by resuming walking. The second group took significantly longer to resume

walking after the heat shock, and demonstrated a markedly lower walking speed after the conditioning period. Based on the data, the authors of the study concluded that the second group of flies had adopted a state of learned helplessness, and therefore decreased their walking efforts.

In our study, we investigated whether learned helplessness in *Drosophila* and its associated decrease in activity induced by heat shocks correlate with neural pathways that modulate stress and reward neurotransmitters. We confined the flies to the bottoms of plastic test tubes and separated them into two groups. One group was immersed in their tubes in a warm water bath for 30 seconds, then set aside for two minutes. This procedure was repeated 10 times, three times a day. A second group was placed in an incubator during the immersion of the first group. The entire procedure was performed for both virgin females and young males. Upon extraction of RNA from fly heads, generation of complementary DNA, and quantitative PCR, the female and male groups were found to have had opposite reactions to the heat stress in terms of gene expression. The female heated group, in comparison to the non-heated group, showed a significant increase in expression of the *dh44* gene, which encodes for regulation of the *dh44* stress hormone, as well as the *GABA* and *NPF* receptor genes, which encode for receptors that are crucial for reward pathways in the fly brain (Figure 1). It should be noted that this is the first study to observe elevated levels of *dh44* in heat-stressed females in *Drosophila*.

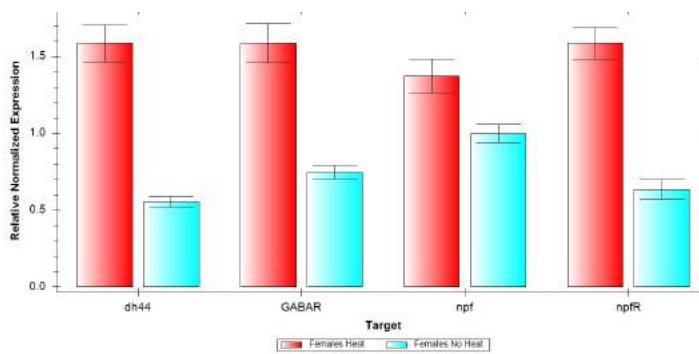


Figure 1. Gene expression levels in virgin female *Drosophila*

The male group, in contrast, showed even more significant differences in expression of these 3 genes, as well as the *dh44* receptor gene, but with the opposite result. Non-heated males exhibited drastically higher levels of gene expression than heated males (Figure 2).

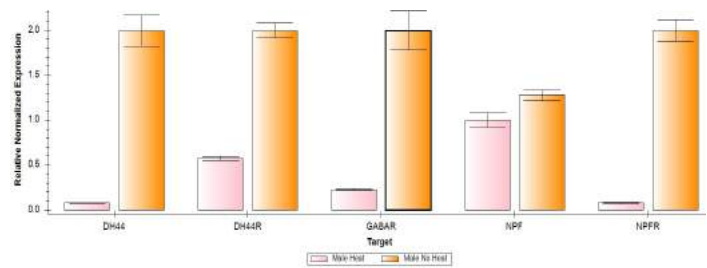


Figure 2. Gene expression levels in young male *Drosophila*

Notably, however, neither the female nor the male group showed statistically significant differences in levels of the *NPF*, which encodes for regulation of the *NPF* reward neuropeptide. This seems to indicate that the experimental conditions for both groups were sufficiently similar, allowing us to rule out the possibility that a major systematic error accounts for the results. We suggest that males may have greater sensitivity to heat stress and therefore “shut down” their stress response system when they learn that the stress is beyond their control. Such a shutdown may be the key to learned helplessness, because it explains the decrease in activity characteristic of that state. This understanding of learned helplessness obviously requires further experimentation and research for support, but nonetheless provides a novel window on the relationship between this kind of stress and depression in animals and possibly humans as well.

Subretinal Implants and Perceptual Learning as Methods of Sight Restoration

Michael Seleski

Advised under Dr. Yossi Mandel and PhD student Tamar Arens-Arad

Phototransduction is the process where photoreceptors, such as rod and cone cells, in the retina convert light into electrical impulses that are sent via the optic nerve to the visual cortex in brain. In scotopic conditions (darkness), photoreceptors are depolarized and release glutamate to interact with horizontal and bipolar cells. In photopic conditions (light), photoreceptors are hyperpolarized, and glutamate is not released. When bipolar cells are depolarized, they will also release glutamate and activate retinal ganglion cells. The retinal ganglion cells can relay the signal to the optic nerve which eventually sends the signal to be processed by the brain.

Retinitis pigmentosa (RP) and age-related macular degeneration (AMD) are two retinal degenerative dis

Life Sciences: Human Biology

eases that can lead to blindness due to the loss of photoreceptors. In these diseases, the other retinal neurons still maintain functionality. A prosthetic retina can be surgically implanted in the subretinal space of the retina to restore vision to blind patients. The implant is an array of photovoltaic electrodes which convert light into electrical impulses. In this prosthesis, a goggles-mounted camera captures the scene and converts the image into a Near-Infrared (NIR) stimulation pulse. A laser pulses the image through the eye onto the implant. The implant converts light into an electrical impulse, subsequently stimulating the other retinal neurons. While some vision is restored, the image is still blurred due to low pixel resolution, non-selectivity of ON and OFF pathways, and other factors.

Based on recent discoveries regarding the brain's plasticity and perceptual learning, visual performance can be improved by training the brain to effectively interpret poor quality images. In this study, rats were used to study the quality of vision before and after implantation of the prosthesis and also possible methods of therapy to further improve vision after implantation of the artificial retina.

Visual evoked potentials (VEPs) were used to assess the functionality of visual pathways in anesthetized and awake rats. VEP signals are electrical signals detected in the visual cortex which resulted from stimulating the visual pathway. VEP signals contain several peaks: N1, P1, N2, P2, and N3 (Figure 1). An increase in the average peak-to-peak amplitude would indicate increased electrical activity in the brain and a higher level of visual acuity.

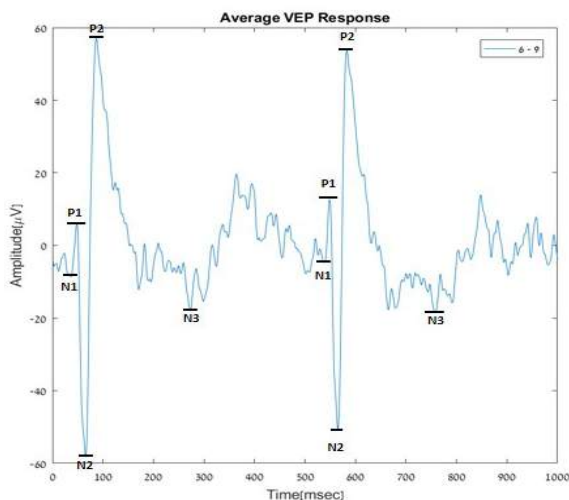


Figure 1. VEP signal for the 6 - 9 minute interval from Day 1 of training. The five peaks, N1, P1, N2, P2, and N3 are shown for two averaged 500 millisecond intervals.

An alternating grating stimulus (reversing the dark and light patterns of the stimulus) was used to stimulate the retina of anesthetized rats (Figure 2). Rats were placed 20 cm away from the stimulus, and the pattern was set to 0.1 cycles per degree (CPD). VEPs were recorded using an AlphaLab SnR for 30 minutes and averaged into ten time intervals, each containing two sets of peaks for 500 milliseconds. This procedure was continued for five consecutive days.

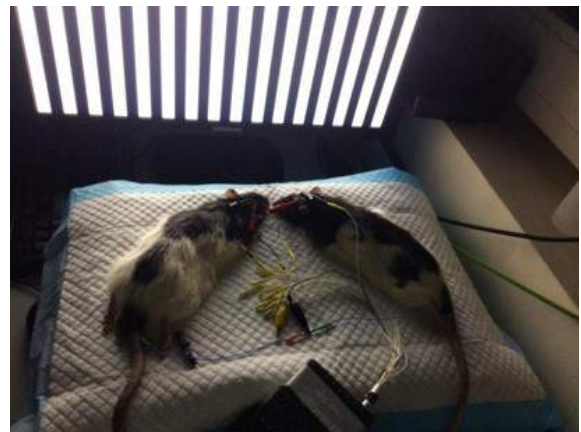


Figure 2. Anesthetized rat watching an alternating grating stimulus. Electrodes are inserted in the scalp overlaying the visual cortex.

The points on the peaks were plotted, and the average N2P2 amplitudes were then calculated and graphed (Figure 3).

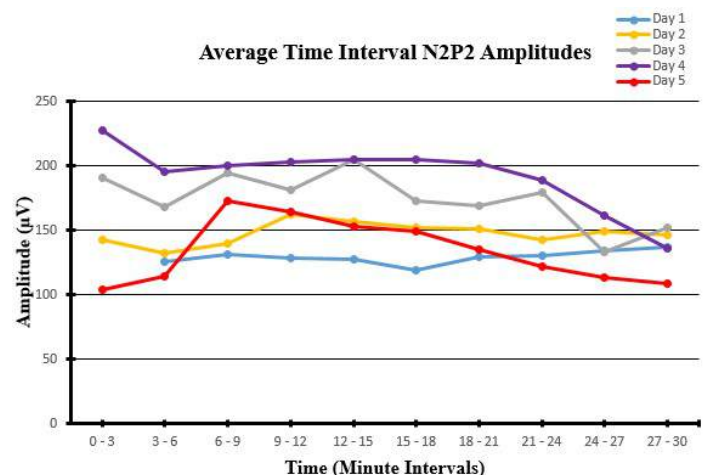


Figure 3. Graph of the average N2P2 amplitudes for ten time intervals over the course of thirty minutes.

After each day, the rat's N2P2 amplitude was expected to increase because of its training. The data in the graph does not accurately support this because there is no definite increasing trend in N2P2 amplitude. One possible explanation for this is because the rat may have had varying levels of anesthesia while recording. Measuring VEP in awake and behaving rats

may provide better results and prove the expected trend. By using a head-mounted projector to stimulate the retina, measurements in awake and behaving rats may be possible. When it is verified that rats can be trained to increase visual acuity, this will be tested in rats with a prosthetic retina as well.

p53-Mediated Regulation of Transcriptional Reprogramming During Carcinogenesis

Azriel Teitelbaum

Advised under Dr. Ofir Hakim in collaboration with Dr. Michal Schwartz

Carcinogenesis is often produced as a result of altered gene expression, a process regulated through transcription factors located in the topologically associated domain of the gene. This study looked at the transcription factor p53 as a potential transcription factor crucial to carcinogenic transcriptional reprogramming by evaluating differences in the accessibility of regulatory regions associated with altered gene expression between carcinogenic and non-tumorigenic cells.

Experiments were run on non-tumorigenic MCF10A mammary epithelial cells and on a transformed in-vitro model of these cells in which an H_Ras oncogene is over-expressed, leading to changes of irregularity regarding quantities of genes expressed and affected. ATAC-seq experiments were performed to map open regulatory sites and RNA-seq experiments were done to identify changes in gene expression in the parental MCF10A cells and in the H_Ras-transformed MCF10A cells. Analysis of these datasets showed that a large amount of the regulatory sites in the MCF10A parental cells, which are located near genes expressed to different degrees in the two types of cells, contained DNA sequence motifs that commonly bind to the p53 tumor suppressor protein. Open regulatory sites in the overexpressed Ras cells by those same genes did not display the same magnitude of motifs with the propensity to bind p53. Additional experiments were then conducted to determine

if reduced levels of p53 were observed in the transformed oncogenic cells. However, results of RNA levels of p53 measured by RNA-seq and qPCR, and protein levels of p53, measured through western blotting, indicated that there was no difference in p53 expression in the carcinogenic cells. Further experimentation, run through immunofluorescence, displayed that cellular localization of p53 is similar in both the innocuous parental and carcinogenic cells, with larger amounts contained in the nucleus and a less dense concentration scattered throughout the cytoplasm (see Figures 1-2.)

Figures 1-2. Immunofluorescence of p53 (Red dye represents stained p53 protein. Blue dye represents stained cell nucleus.)

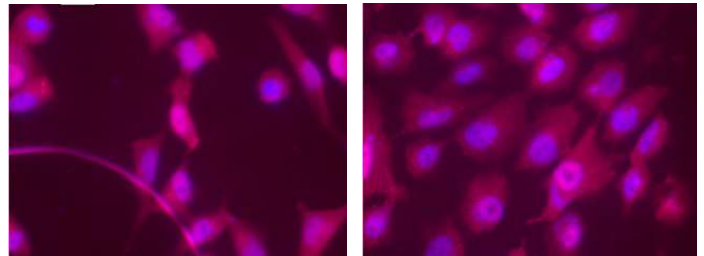


Figure 1

Figure 1. Over-expressed H_Ras oncogenic cell

Figure 2

Figure 2. MCF10A parental cell

Though additional experimentation is necessary and underway, there are currently several theories that explain the increased quantity of p53 binding motifs in MCF10A cell regulatory sites by the incongruously expressed genes, despite the equal amounts of the p53 protein and RNA expressed in both cells. One possibility is that the motifs found by the regulatory sites are not specifically for p53; and that another transcription factor sharing the motif is really the source of the difference in gene expression. As such, ChIP-sequencing is currently being run to determine the exact identity of the transcription factors bound to the regulatory sites located by those genes in the parental cells. Alternatively, those motifs do bind p53 in the MCF10A cells, however, the p53 expressed in the H_Ras-overexpressed cells either binds elsewhere in the transformed cells genome or possibly doesn't bind its full quantity to specific sites in the chromatin.